AD-A160 015 AN ANALYSIS OF THE TENSOR DIELECTRIC CONSTANT OF SEA ICE AT MICROWAVE FREQUENCIES(U) AEROJET ELECTROSYSTEMS CO AZUSA CA A STOGRYN OCT 85 AESC-7975 1/1

UNCLASSIFIED N00014-83-C-0726 F/G 8/12 NL

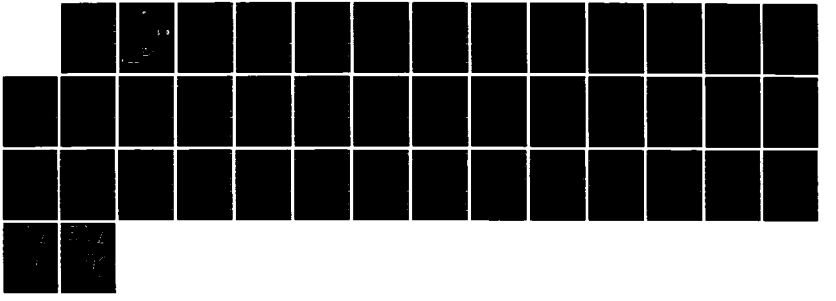

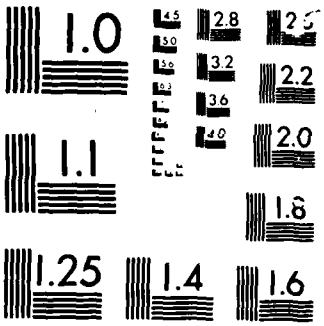

MICROCOPY CHART

AN ANALYSIS OF THE TENSOR DIELECTRIC CONSTANT OF SEA ICE AT MICROWAVE FREQUENCIES

CONTRACT NO. N00014-83-C-0726

PREPARED FOR

OFFICE OF NAVAL RESEARCH
DEPARTMENT OF THE NAVY
ARLINGTON, VIRGINIA 22217

REPORT 7975

OCTOBER, 1985

AEROJET
ELECTROSYSTEMS
COMPANY

AZUSA, CALIFORNIA

AN ANALYSIS OF THE TENSOR DIELECTRIC CONSTANT OF SEA ICE AT MICROWAVE FREQUENCIES

Final Report

October, 1985

Report 7975

Contract No. N00014-83-C-0726

by

A. Stogryn

Prepared for

OFFICE OF NAVAL RESEARCH
DEPARTMENT OF THE NAVY
Arlington, Virginia 22217

Prepared by

AEROJET ELECTROSYSTEMS COMPANY
1100 West Hollyvale Street
Azusa, California 91702

INTRODUCTION AND SUMMARY

Aerojet ElectroSystems Company has been performing research for the Office of Naval Research on a number of topics in electromagnetic theory of interest in explaining the microwave radiometric characteristics of sea ice. Under Contract N00014-81-C-0553 (see Report 6140 published in December 1981 and the Final Report 7788 published in March 1985) the bilocal approximation in strong fluctuation theory was developed and applied to isotropic random media such as snow. The work reported on here and funded under Contract N00014-83-C-0726 is an extension of these ideas to the anisotropic case which is characteristic of most forms of sea ice. Specifically this study has concentrated on deriving equations for computing the tensor dielectric constant of sea ice and making comparisons of the computations with published measurements on various components of the dielectric tensor (as well as attenuation coefficients, which are closely related to the dielectric constant).

The theory is shown to be able to account quantitatively for large parts of the published experimental data on a variety of ice types in the frequency range 0.1 to 40 GHz and temperatures from -5 to -30°C. A few discrepancies, however, are noted. It is not known whether further development of the theory will be required to resolve these differences between theory and experiment or whether the experiments themselves must be refined. It is well known that accurate dielectric constant measurements on sea ice present some rather difficult experimental problems. Some inconsistencies within the existing body of experimental data itself are pointed out in this work.

CONTENTS

ILLUSTRATIONS

AN ANALYSIS OF THE TENSOR DIELECTRIC CONSTANT OF SEA ICE AT MICROWAVE FREQUENCIES

I. INTRODUCTION

Sea ice is an interesting and complex substance of considerable importance for remote sensing studies of the earth. An essential ingredient of any attempt to achieve a quantitative understanding of the microwave radiometric and radar signatures of the diverse types of naturally occurring sea ice is a knowledge of the dielectric properties of the ice. A summary of experimental work on the dielectric constant involving both artificial and natural sea ice may be found in [1]. To this may be added the work of Bogorodskii and Khokhlov [2] which emphasizes work performed in the Soviet Union. Further experiments are currently underway. However, the highest frequency which appears to have been investigated experimentally is still below the 40 GHz limit already discussed in [1] and [2].

The attempts to analyze the results of these experiments have ranged from linear regression models [1], [3], Wiener's dielectric mixing formula [3] and a simple averaging formula for spherical inclusion [4], to more sophisticated models which explicitly recognize the fact that sea ice, at least in some of its forms, should be anisotropic due to the elongated brine cells which it contains. In the latter category are the formulas based on Vant's dissertation discussed in [1] and a variant due to Farrelly [5].

All of these formulas are strictly limited because scattering effects due to the random brine cells and air pockets in the ice are not treated. Thus, for example, they are not well suited for studying

multi-year ice at frequencies above 20 GHz because of the dominant role played by scattering from air bubbles. It is the intent of this work to extend the methods of strong fluctuation theory, which has already been developed for isotropic random media [6], to calculate the dielectric constant of an anisotropic medium such as sea ice. By using this approach, scattering effects are included. Improvements compared to previously calculated behavior are obtained even at frequencies as low as 0.1 GHz. This is partly due to the fact that the strong fluctuation result for the quasi-static dielectric constant does not agree with Tinga's formula which was used by Vant and Farrelly and partly the result of the greater flexibility which strong fluctuation theory allows in specifying the statistical properties of the brine cells. It is not limited to assuming elliptically shaped cells as was necessary in [1] and [5].

II. PHYSICAL MODEL OF SEA ICE

The model to be discussed here assumes that sea ice is a mixture of pure ice, brine, and air. The pure ice occurs in the form of thin platelets of the order of 0.5 mm thick with the crystallographic c-axis perpendicular to the plane of the platelets [7]. These platelets are stacked together to form grains whose average cross sectional diameter is about 0.4 cm near the surface of the ice and increases linearly by 1 cm for every 30 cm of depth [8]. The c-axis of the grains can have various orientations. For frazil, the axis may be assumed to be randomly oriented [1] while for columnar ice there is a tendency for the polar angle of the c-axis (measured from the vertical) to increase from approximately 0° near the surface to 90° as the depth increases. The azimuthal orientation of the c-axis was taken to be random in this study. This imposes a certain symmetry on the dielectric

tensor which will hold in most, but not all, cases of interest and excludes ice formed in the presence of strongly directional currents.

The brine cells in the model were assumed to occur between the platelets comprising a grain and are thus perpendicular to the c-axis. Structures such as brine drainage channels were ignored. Within a grain the brine cells occur as long, roughly cylindrical, parallel inclusions with random spacings. The radius of these cells is of the order of 0.025 mm [7] while their length varies from 3 mm [1] to over 1 cm [7].

For purposes of the model, air pockets in the ice are assumed to occur only between the ice grains. Thus, the grains consist of only brine and ice. For lack of more definitive information the air bubbles are assumed to be roughly spherical in shape so that they may be described by a spherically symmetric correlation function.

In order to calculate the dielectric properties of sea ice, it is necessary to specify the dielectric constants of the constituents as well as their respective volume fractions. For this study the dielectric constant equations discussed in [9] for pure ice and in [10] for brine in sea ice were used while the dielectric constant of air was taken to be one. Assuming a mean density $\rho_{ice} = 0.926$ g/cm^3 [8] for bubble-free sea ice, the volume fraction of pure ice is

$$v_{ice} = (\rho - \rho_b v_b)/\rho_{ice} \qquad (1)$$

where ρ is the density of the sea ice sample under consideration, ρ_b the density of brine, and v_b the volume fraction of brine. The volume fraction of air is

$$v_{air} = 1 - v_b - v_{ice} \tag{2}$$

A fit to the data of Nelson [11] yields

$$\rho_b = 1.02814 - 0.88128\times10^{-2}t - 0.9298\times10^{-4}t^2 \quad g/cm^3 \tag{3}$$

in the temeprature range $-1 \geq t \geq -54°C$. The brine volume may be expressed as

$$v_b = Sp \tag{4}$$

where S is the ice salinity (absolute, not parts per thousand) and p is a function of temperature which has been tabulated in [8]. For numerical work the fit

$$p = \begin{cases} -2.28 - 52.56\ t^{-1} & \text{if } t \geq -2.06°C \\ 0.930 - 45.917\ t^{-1} & \text{if } -2.06 > t \geq -8.2°C \\ 1.189 - 43.795\ t^{-1} & \text{if } -8.2 > t \geq -22.9°C \\ 21.9921 + 2.96856\times10^{3}t^{-1} + 1.53039\times10^{5}t^{-2} + 3.502798\times10^{6}t^{-3} \\ \qquad + 3.0401\times10^{7}t^{-4} & \text{if } -22.9 > t \geq -36.8°C \\ 2.8167 + 0.9494\times10^{-1}t + 0.9603\times10^{-3}t^{2} \\ \qquad \text{if } -36.8 > t \geq -43.2°C \end{cases} \tag{5}$$

is convenient. The above equations for p in the range $t > -22.9°C$ were first published by Frankenstein and Garner [12].

III. BILOCAL APPROXIMATION FOR THE DIELECTRIC CONSTANT

The use of the bilocal approximation in strong fluctuation theory for a random medium yields the equation [13]

$$\nabla \times \nabla \times \underset{\sim}{E}^m - k_o^2 \underset{\approx}{K}_o \underset{\sim}{E}^m - \left\langle \underset{\approx}{\xi}\, \underset{\approx}{G}\, \underset{\approx}{\xi} \right\rangle \underset{\sim}{E}^m = 0 \tag{6}$$

for the mean electric field propagating in the medium. Here k_o is the free space propagation constant, $\underset{\approx}{K}_o$ the quasi-static dielectric tensor and $\underset{\approx}{\xi}(\underset{\sim}{r})$ a random tensor defined by

$$\underset{\approx}{\xi}(\underset{\sim}{r}) = \Delta\underset{\approx}{L}[\underset{\approx}{I} + \underset{\approx}{S}\,\Delta\underset{\approx}{L}]^{-1} \tag{7}$$

where

$$\Delta\underset{\approx}{L} = k_o^2(\underset{\approx}{K}_o - \underset{\approx}{K}^r(r)) \tag{8}$$

The tensor $\underset{\approx}{S}$ is the coefficient of the delta function part of the Green's function $\underset{\approx}{\Gamma}$ which satisfies the equation

$$\nabla \times \nabla \times \underset{\approx}{\Gamma} - k_o^2 \underset{\approx}{K}_o \underset{\approx}{\Gamma} = \underset{\approx}{I}\,\delta(\underset{\sim}{r} - \underset{\sim}{r}') \tag{9}$$

and $\underset{\approx}{I}$ is the unit dyad. $\underset{\approx}{K}^r(\underset{\sim}{r})$ in (8) is the random dielectric tensor of the medium. The last term in (6) accounts for the effects of scattering from the random inhomogeneities. Its i^{th} component is given by the principal value integral

$$[\left\langle \underset{\approx}{\xi}\, G\, \underset{\approx}{\xi} \right\rangle \underset{\sim}{E}^m]_i = PV \int d^3r' \left\langle \xi_{ij}(\underset{\sim}{r})\, \xi_{k\ell}(\underset{\sim}{r}') \right\rangle \Gamma'_{jk}(\underset{\sim}{r},\underset{\sim}{r}')\, E_\ell(\underset{\sim}{r}') \tag{10}$$

where $\underset{\approx}{\Gamma}'$ is the kernel of $\underset{\approx}{G}$ and is related to $\underset{\approx}{\Gamma}$ by

$$\underset{\approx}{\Gamma}'(\underset{\sim}{r},\underset{\sim}{r}') = \underset{\approx}{\Gamma}(\underset{\sim}{r},\underset{\sim}{r}') - \underset{\approx}{S}\,\delta(\underset{\sim}{r} - \underset{\sim}{r}') \tag{11}$$

In (10) and below, the summation convention is used for repeated Latin letter subscripts and the angular brackets denote expected value.

If, as in [6], a plane wave

$$\underset{\sim}{E}^m_p = E_o\, \hat{\underset{\sim}{p}}\, \exp[i\,\underset{\sim}{k}\cdot\underset{\sim}{r}] \tag{12}$$

with polarization $\hat{\underset{\sim}{p}}$ is considered in a homogeneous medium and boundary effects are neglected so that $\underset{\approx}{\Gamma}$ becomes an infinite medium Green's function whose argument depends only on the difference $\underset{\sim}{r}-\underset{\sim}{r}'$, it is found that $\underset{\sim}{E}_p^m$ satisfies the wave equation

$$\nabla \times \nabla \times \underset{\sim}{E}_p^m - k_o^2 \underset{\approx}{K} \underset{\sim}{E}_p^m = 0 \tag{13}$$

where the effective dielectric constant $\underset{\approx}{K}$ is

$$\underset{\approx}{K} = \underset{\approx}{K}_o + \frac{1}{k_o^2} \underset{\approx}{E} \tag{14}$$

The scattering contribution $\underset{\approx}{E}$ in (14) is defined by

$$E_{i\ell} = PV\int d^3r' \; C_{ijk\ell}(\underset{\sim}{r} - \underset{\sim}{r}') \; \underset{\approx}{\Gamma}'_{jk}(\underset{\sim}{r} - \underset{\sim}{r}') \exp[-ik\cdot(\underset{\sim}{r}-\underset{\sim}{r}')] \tag{15}$$

where

$$C_{ijk\ell}(\underset{\sim}{r}-\underset{\sim}{r}') = \left\langle \xi_{ij}(\underset{\sim}{r}) \; \xi_{k\ell}(\underset{\sim}{r}') \right\rangle \tag{16}$$

A translation of the origin shows that $\underset{\approx}{E}$ is actually independent of $\underset{\sim}{r}$.

Specific equations for the components of $\underset{\approx}{K}_o$ and $\underset{\approx}{E}$ will be developed later. However, on the basis of the physical model discussed above, the general structure of the dielectric tensor $\underset{\approx}{K}$ can be described. If the z axis is chosen to be vertical, the random azimuthal orientation of the c axes of the ice grains implies that $\underset{\approx}{K}_o$ is invariant under rotations about the unit vector $\hat{\underset{\sim}{z}}$ and reflections in any plane containing the z axis. Thus $\underset{\approx}{K}_o$ is necessarily a diagonal tensor of the form

$$\underset{\approx}{K}_o = \text{diag}(K_{01}, K_{01}, K_{03}) \tag{17}$$

The situation for $\underset{\approx}{K}$ is somewhat more complicated because of the occurrence of the propagation vector $\underset{\sim}{k}$ in (15). If $\underset{\sim}{k}$ were zero, then $\underset{\approx}{K}$ would have the same structure as $\underset{\approx}{K}_o$. However, since we are interested in finite

particle size to wavelength ratios, additional components are not excluded in $\underline{\underline{K}}$ - namely, additive terms proportional to $\underline{k}\underline{k}$, $\underline{k}\underline{z}$, and $\underline{z}\underline{k}$ each of which are form invariant under the above-mentioned transformations. One may conclude that the coefficients of $\underline{k}\underline{z}$ and $\underline{z}\underline{k}$ are identical because $\underline{\underline{E}}$ in (15) is a symmetric tensor as a result of the symmetry of C in its first two and last two indices and the fact that the infinite medium Green's function is symmetric. Let the y axis be chosen so that $\underline{k}$ lies in the $\hat{\underline{x}}$-$\hat{\underline{z}}$ plane:

$$\underline{k} = (k_x, 0, k_z) \tag{18}$$

Then these considerations show that $\underline{\underline{K}}$ is of the form

$$\underline{\underline{K}} = \begin{pmatrix} K_{11} & 0 & K_{13} \\ 0 & K_{22} & 0 \\ K_{13} & 0 & K_{33} \end{pmatrix} \tag{19}$$

where each of the components are functions of k_x and k_y . Furthermore, K_{13} vanishes if either k_x or k_z in (18) is equal to zero.

In typical applications, one of the components of $\underline{k}$ is known. The value of $\underline{\underline{K}}(\underline{k})$ may be computed after solving a dispersion equation for the unknown component of $\underline{k}$. The latter is obtained from substituting (12) into (13). If $\hat{\underline{p}} = \hat{\underline{y}}$, then

$$k^2 - k_o^2 K_{22}(\underline{k}) = 0 \tag{20}$$

The solution of this equation yields the effective dielectric constant for the ordinary wave. If $\hat{\underline{p}}$ lies in the $\hat{\underline{x}}$-$\hat{\underline{z}}$ plane, the extraordinary wave is determined by the determinantal equation

$$\begin{vmatrix} k^2 - k_x^2 - K_{11} & -k_x k_z - k_o^2 K_{13} \\ -k_x k_z - k_o^2 K_{13} & k^2 - k_z^2 - k_o^2 K_{33} \end{vmatrix} = 0 \tag{21}$$

To carry out this program, it remains to specify the components of $\underset{\approx}{K}$ more explicitly. The quasi-static and scattering contributions to $\underset{\approx}{K}$ for sea ice are treated below.

IV. THE QUASI-STATIC DIELECTRIC CONSTANT

In the model of sea ice the quasi-static dielectric constant $\underset{\approx}{K}_o$ is computed in two stages. First, an expression is found for the equivalent dielectric constant of the grains described in Section II and secondly this expression is used to compute the quasi-static dielectric constant of the ice as a whole taking into account the arbitrary orientations of the c axes of the grains and the air bubbles.

For an individual grain, let us choose a coordinate system x', y', z' oriented so that the brine cells are parallel to z'. The quasi-static dielectric tensor

$$\underset{\approx}{K}' = \text{diag}(K_1, K_1, K_3) \tag{22}$$

of this grain is determined according to strong fluctuation theory by the equation [6]

$$\left\langle \underset{\approx}{\xi}_{\text{grain}} \right\rangle = 0 \tag{23}$$

where $\underset{\approx}{\xi}_{\text{grain}}$ is determined by equations of the form (7) and (8) with $\underset{\approx}{K}_o$ replaced by $\underset{\approx}{K}'$ and, since the grain is assumed to be a two-component medium consisting of pure ice and brine, the random tensor $\underset{\approx}{K}^r$ reduces to a random scalar multiple of the unit dyad which may assume the values K_{ice} or K_{brine} (the dielectric constants of ice and brine respectively). Thus, in (23), the expected value reduces to a sum of two terms weighted according to $v_{ice}/(v_b+v_{ice})$ and $v_b/(v_b+v_{ice})$ which are the respective probabilities of a point being in ice or brine.

The tensor $\underset{\approx}{S}_q$ to be used in (23) and corresponding to $\underset{\approx}{S}$ in (7) depends on the geometry of the brine cells. Specific formulas are discussed in [14]. Because of the axial symmetry of the brine cells, $\underset{\approx}{S}_q$ is diagonal of the form

$$\underset{\approx}{S}_q = \text{diag}(S_{g1}, S_{g2}, S_{g3}) \tag{24}$$

with

$$S_{g3} = -(k_o^{-2} + 2K_1 S_{g1})/K_3 \tag{25}$$

If the equi-correlation surface is assumed to be defined by the ellipsoid

$$(x'^2+y'^2)/\ell_\rho^2 + z'^2/\ell_z^2 = \text{constant} \tag{26}$$

then

$$S_{g1} = -[(1 + e^2)\tan^{-1}e - e]/(2k_o^2 K_1 e^3) \tag{27}$$

where

$$e = [(\ell_\rho^2 K_3)/(\ell_z^2 K_1) - 1]^{1/2} \tag{28}$$

This choice corresponds somewhat to the model of elliptic inclusions developed in [1] and [5] if the correlation lengths ℓ_ρ, and ℓ_z are assumed to be proportional to the radius and length of a mean brine cell. It will be seen later that this is not the most satisfactory choice for the equi-correlation surface. In fact, the roughly cylindrical shape of the brine cells suggest that an equi-correlation surface

$$(x'^2+y'^2)^{1/2}/\ell_\rho + |z'|/\ell_z = \text{constant} \tag{29}$$

may be more realistic. Using the formulas of [14], this assumption yields

$$S_{g1} = -\left[-2a^{-1/2}\,\ell n[a^{1/2} - 1] - 1 + [a - 1]^{1/2}\right]\ell_z / [2\ell_\rho\, a\, k_o^2 (K_1 K_3)^{1/2}] \tag{30}$$

where

$$a = 1 + (K_1 \ell_z^2)/(K_3 \ell_\rho^2) \tag{31}$$

The study in [15] indicates that ℓ_z and ℓ_ρ should be proportional to the length and radius of a mean brine cell. On the basis of the data in Section II, the ratio ℓ_z/ℓ_ρ should be larger than 100.

After $\underset{\approx}{K}'$ has been determined according to the above procedure, a second application of the prescriptions of strong fluctuation theory leads to the quasi-static dielectric constant of sea ice which is treated as consisting of ice grains and air bubbles. To accomplish this, it is necessary to use the standard x,y,z coordinate system oriented with the z axis vertical. In this coordinate system, the grain dielectric constant becomes $\underset{\approx}{K}_g^r$ which is related to $\underset{\approx}{K}'$ by

$$\underset{\approx}{K}_g^r = \underset{\approx}{A}^{-1} \underset{\approx}{K}' \underset{\approx}{A} \tag{32}$$

where $\underset{\approx}{A}$ is the matrix transforming from the standard coordinate system to the prime system. Introducing Euler angles θ_B, ϕ_B, ψ_B, where the conventions of [16] are used, and noting that ψ_B may be set equal to zero because of the assumed axial symmetry of the brine cells about the z' axis, A is given by

$$A = \begin{pmatrix} \cos\phi_B & \sin\phi_B & 0 \\ -\cos\theta_B\sin\phi_B & \cos\theta_B\cos\phi_B & \sin\theta_B \\ \sin\theta_B\sin\phi_B & -\sin\theta_B\cos\phi_B & \cos\theta_B \end{pmatrix} \tag{33}$$

where θ_B is the angle between the axis of the brine cells in a grain and the vertical and ϕ_B describes the azimuthal position. Note that $\underset{\approx}{K}_g^r$ is random because these angles are random.

The equation $\langle \underset{\approx}{\xi} \rangle = 0$ which determines the quasi-static dielectric constant [6] of sea ice may be written

$$v_{air}\underset{\approx}{\xi}_{air} + v_{qrain}\bar{\underset{\approx}{\xi}}_{q} = 0 \tag{34}$$

where v_{air} is given by (12) and v_{qrain} is the sum of v_b and v_{ice}. These quantities are the probabilities of a point being in the air bubbles or grains respectively. The tensors $\underset{\approx}{\xi}$ in (34) are of the form shown in (7) and (8). In the case of $\underset{\approx}{\xi}_{air}$, $\underset{\approx}{K}^r = \underset{\approx}{I}$ in (8). Here, and below, the symbol $\bar{}$ represents an average over the angles θ_B and ϕ_B so that $\bar{\underset{\approx}{\xi}}_q$ is the angular average of $\underset{\approx}{\xi}_q$ which is determined by (7) and (8) if (32) is used for $\underset{\approx}{K}^r$. The air bubbles are assumed to be roughly spherical and hence described by a spherically symmetric correlation function. Thus $\underset{\approx}{S}$ will be a diagonal tensor

$$\underset{\approx}{S} = \mathrm{diag}(S_1, S_1, S_3) \tag{35}$$

of the form (25)-(28) with the substitutions $K_1 \rightarrow K_{01}$, $K_3 \rightarrow K_{03}$, and the restriction $\ell_\rho = \ell_z$. With this expression for $\underset{\approx}{S}$ a routine computation shows that the components of $\underset{\approx}{\xi}_q$ are

$$\xi_{q11} = \left| \alpha_1\gamma - \alpha_1\alpha_3 + [S_1S_3\beta\cos^2\phi_B + \alpha_3S_1\cos^2\phi_B - \alpha_1S_3] \right. \\ \left. \beta\sin^2\theta_B \right| / (S_1\alpha_1\gamma) \tag{36a}$$

$$\xi_{q22} = \left| \alpha_1\gamma - \alpha_1\alpha_3 + [S_1S_3\beta\sin^2\phi_B + \alpha_3S_1\sin^2\phi_B - \alpha_1S_3] \right. \\ \left. \beta\sin^2\theta_B \right| / (S_1\alpha_1\gamma) \tag{36b}$$

$$\xi_{q33} = \left| \gamma - \alpha_1 + S_1\beta\sin^2\theta_B \right| / (S_3\gamma) \tag{36c}$$

$$\xi_{q12} = \xi_{g21} = \beta[\alpha_3 + S_3\beta] \sin^2\theta_B \cos\phi_B \sin\phi_B/(\alpha_1\gamma) \quad (36d)$$

$$\xi_{q13} = \xi_{g31} = -\beta\cos\theta_B \sin\theta_B \sin\phi_B/\gamma \quad (36e)$$

$$\xi_{q23} = \xi_{q32} = \beta\cos\theta_B \sin\theta_B \cos\phi_B/\gamma \quad (36f)$$

where

$$\alpha_i = 1 + k_o^2 S_i(K_{oi} - K_i) \qquad (i = 1 \text{ or } 3) \quad (37a)$$

$$\beta = k_o^2(K_3 - K_1) \quad (37b)$$

$$\gamma = \alpha_1\alpha_3 + (\alpha_1 S_3 - \alpha_3 S_1 - S_1 S_3\beta)\beta\sin^2\theta_B \quad (37c)$$

Part of the average to obtain $\bar{\bar{\xi}}_g$ from these equations is easy to perform. The assumption of equally probable azimuthal orientations of the c axis is equivalent to integrating over ϕ_B and dividing by 2π. This immediately yields a diagonal tensor

$$\bar{\bar{\xi}}_g = \text{diag}(\bar{\xi}_{q1}, \bar{\xi}_{q1}, \bar{\xi}_{q3}) \quad (37)$$

However, the θ_B average depends on introducing a probability distribution $P(\theta_B)$ for the brine axis angle before integrating. For all types of ice except frazil, which will be treated below, a lack of knowledge of $P(\theta_B)$ precludes a rigorous integration. To circumvent this difficulty the mean value theorem may be applied. This is equivalent to treating θ_B as a parameter representing an appropriate average brine cell angle. Thus $\bar{\bar{\xi}}_q$ may be evaluated from (36a)-(36c) after replacing $\cos^2\phi_B$ and $\sin^2\phi_B$ by 1/2.

For frazil, where all orientations of the c axis are equally probable, $P(\theta) = 1/2$. In this case, the complete symmetry requires $\underset{\approx}{K}_o$, $\underset{\approx}{S}$, and $\underset{\approx}{\bar{\xi}}_q$ to be scalar multiples of the unit dyad (denoted by K_{of}, S_f and $\bar{\xi}_f$ respectively. Remembering that the element of solid angle is $\sin\theta_B d\theta_B$ (the ϕ_B integration has already been performed), it is found that

$$\bar{\xi}_f = k_o^2 \Big\{ 2(K_{of} - K_1)[1 + k_o^2 S_f (K_{of} - K_1)]^{-1} + (K_{of} - K_3)[1 + k_o S_f (K_{of} - K_3)]^{-1} \Big\} / 3 \qquad (38)$$

With either of these expressions for $\underset{\approx}{\bar{\xi}}_q$ in (34) the quasi-static dielectric constant may be found. A numerical solution is necessary.

V. SCATTERING TERMS

The scattering contribution $\underset{\approx}{E}$ to the effective dielectric constant $\underset{\approx}{K}$ in (14) will now be considered. Scattering within a grain is neglected because of the very small diameters and close spacing of the brine cells within the grain compared to the wavelengths of interest. Thus, the sea ice is treated as a two-component material consisting of grains with dielectric constant (32) and air bubbles. The scattering correction depends only on scattering from the air bubbles and scattering from the grains due to the fact that the dielectric tensors describing the individual grains have randomly oriented principal axes corresponding to randomly oriented grain c axes.

There are three factors to be considered in evaluating (15). These are the specifications of $C_{ijk\ell}$, Γ'_{jk}, and the evaluation of the principal value integral. First consider the fourth rank correlation tensor (16). Following the method discussed in [15], $\underset{\approx}{\xi}$ is written as

$$\underset{\approx}{\xi}(\underset{\sim}{r}) = \underset{\approx}{\xi}_{air}\, H(\underset{\sim}{r}) + \underset{\approx}{\xi}_{q}\,[1 - H(\underset{\sim}{r})]$$

$$= \underset{\approx}{\xi}_{air}\, H(\underset{\sim}{r}) + \underset{\approx}{\bar{\xi}}_{q}\,[1 - H(\underset{\sim}{r})] + (\underset{\approx}{\xi}_{q} - \underset{\approx}{\bar{\xi}}_{q})[1 - H(\underset{\sim}{r})] \qquad (39)$$

where $H(\underset{\sim}{r})$ is a random function equal to one if $\underset{\sim}{r}$ is in an air bubble and zero if $\underset{\sim}{r}$ is in a grain. When forming $C_{ijk\ell}$ the first two terms in the second line of (39) are evaluated exactly as in [15]. The third term does not lead to cross products with the first two terms when expected values are taken so that

$$C_{ijk\ell}(\underset{\sim}{r}-\underset{\sim}{r}') = [\xi_{air\,ij}\,\xi_{air\,k\ell} + \bar{\xi}_{qij}\,\bar{\xi}_{qk\ell} - \xi_{air\,ij}\,\bar{\xi}_{qk\ell}$$

$$- \bar{\xi}_{q\,ij}\,\xi_{air\,k\ell}]R_a(\underset{\sim}{r} - \underset{\sim}{r}') + B_{ijk\ell}(\underset{\sim}{r}_2 - \underset{\sim}{r}_1) \qquad (40)$$

In (40)

$$B_{ijk\ell}(\underset{\sim}{r}_2-\underset{\sim}{r}_1) = \left\langle [\xi_{q\,ij}(1)\xi_{q\,k\ell}(2) - \bar{\xi}_{q\,ij}\,\bar{\xi}_{q\,k\ell}][1 - H(\underset{\sim}{r}_1)][1 - H(\underset{\sim}{r}_2)]\right\rangle \qquad (41)$$

with the arguments 1 and 2 in $\underset{\approx}{\xi}_{q}$ referring to the Euler angles and R_a is a scalar function describing the air bubble statistics [15]. It will be assumed that the air bubbles have an exponential correlation function so that [15]

$$R_a(\underset{\sim}{r}_2-\underset{\sim}{r}_1) = v_{air}(1 - v_{air})\exp[-|\underset{\sim}{r}_2-\underset{\sim}{r}_1|/\ell_a] \qquad (42)$$

where the correlation length ℓ_a is related to the mean bubble diameter d_a by

$$\ell_a = \frac{2}{3}\,(1 - v_{air})\,d_a \qquad (43)$$

The term $B_{ijk\ell}$ in (40) is considerably more complex and much data on ice remains to be analyzed to determine its precise behavior. However, it is obvious that $B_{ijk\ell}$ approaches zero as $|\underset{\sim}{r}_2-\underset{\sim}{r}_1|$ becomes large. The ad-hoc assumption will be made that

$$B_{ijk\ell}(\underline{r}_2-\underline{r}_1) = B_{ijk\ell}(0)\exp[-|\underline{r}_2-\underline{r}_1|/\ell_q] \tag{44}$$

From (40), $B_{ijk\ell}(0)$ is evaluated as

$$B_{ijk\ell}(0) = [\overline{\xi_{g\,ij}\,\xi_{g\,k\ell}} - \bar{\xi}_{g\,ij}\,\bar{\xi}_{g\,k\ell}]v_{grain} \tag{45}$$

According to the overlap picture discussed in [15] it is expected that the correlation length ℓ_q will be somewhat less than the mean grain diameter d_g. It will be assumed to be given by

$$\ell_q = \frac{2}{3}\,d_g \tag{46}$$

The second term in (45) has already been evaluated in (36)-(37). Before writing equations for the first term, it is useful to note the symmetries of $B_{ijk\ell}$. $B_{ijk\ell}(0)$ is symmetric under the interchange of i and j, k and ℓ, and the pair $(ij) \longleftrightarrow (k\ell)$ as can be seen by examination of (36). Further, the basic assumption of invariance under orthogonal transformations leaving the z axis fixed holds. All of these symmetries combined reduce the total number of independent components to only five. In fact, it is found that

$$\begin{aligned} B_{ijk\ell}(0) = {} & a_1\,\delta_{ij}\,\delta_{k\ell} + a_2[\delta_{ik}\,\delta_{j\ell} + \delta_{i\ell}\,\delta_{jk}] + b_1[\delta_{ij}\,\delta_{k3}\,\delta_{\ell 3} \\ & + \delta_{k\ell}\,\delta_{i3}\,\delta_{j3}] + b_2[\delta_{ik}\,\delta_{j3}\,\delta_{k3} + \delta_{i\ell}\,\delta_{j3}\,\delta_{k3} + \delta_{jk}\,\delta_{i3}\,\delta_{\ell 3} \\ & + \delta_{j\ell}\,\delta_{i3}\,\delta_{k3}] + c_1\,\delta_{i3}\,\delta_{j3}\,\delta_{k3}\,\delta_{\ell 3} \end{aligned} \tag{47}$$

where the δ's are the Kronecker deltas and the constants are

$$a_1 = B_{1122}(0) \tag{48a}$$

$$a_2 = B_{1212}(0) \tag{48b}$$

$$b_1 = B_{1133}(0) - B_{1122}(0) \tag{48c}$$

$$b_2 = B_{1313}(0) - B_{1212}(0) \tag{48d}$$

$$c_1 = B_{3333}(0) - a_1 - 2a_2 - 2b_1 - 4b_2 \tag{48e}$$

A routine but lengthy computation of the average of the product in (45) may be performed. The average over ϕ_B is simply an integral and, except for frazil, the θ_B average is treated as in Section IV by interpreting θ_B to be a parameter representing a mean brine cell axis angle. For simplicity, this angle is identified with the parameter θ_B appearing in Section IV. With these approximations the result is

$$B_{1122}(0) = \left\{\frac{1}{4}\left[S_3\beta^2 \cos^2\theta_B \sin^2\theta_B/(\alpha_1\gamma)\right]^2 - \bar{\xi}_{a11}\, S_3\beta^2 \cos^2\theta_B \sin^2\theta_B/(\alpha_1\gamma) - \frac{1}{8}[\beta\sin^2\theta_B(\alpha_3 + S_3\beta)/(\alpha,\gamma)]^2\right\} v_{grain} \tag{49a}$$

$$B_{1212}(0) = \frac{1}{8}\left\{\beta \sin^2\theta_B[\alpha_3 + S_3\beta]/(\alpha_1\gamma)\right\}^2 v_{grain} \tag{49b}$$

$$B_{1313}(0) = \frac{1}{2}\left[\beta \cos\theta_B \sin\theta_B/\gamma\right]^2 v_{grain} \tag{49c}$$

$$B_{1133}(0) = B_{3333}(0) = 0 \tag{49d}$$

where the quantities that appear have been defined in equations (34)-38).

As in the case of the quasi-static dielectric constant, frazil may be treated more precisely. In fact, the spherical symmetry implies that $b_1 = b_2 = c_1 = 0$ in (47). Contracting on the two inner and two outer indices in (47) shows that

$$B_{ijji}(0) = 3a_1 + 12a_2 \tag{50}$$

But recalling that $\underset{\approx}{K}_o$, $\underset{\approx}{S}$, and $\underset{\approx}{\bar{\xi}}_a$ are scalar multiples of the unit dyad for frazil allows $B_{ijji}(0)$ to be evaluated using (36) as

$$B_{ijji}(0) = k_o^4 v_{grain}\left\{2(K_{of} - K_1)^2[1 + k_o^2 S_f(K_{of} - K_1)]^{-2} + (K_{of} - K_3)^2[1 + k_o^2 S_f(K_{of} - K_3)]^{-2}\right\} - 3\bar{\xi}_f^{\,2} v_{grain} \tag{51}$$

Further, a_2 in (47b) may be evaluated exactly by integrating (49b) after multiplying by $\frac{1}{2}\sin\theta_B$. The result is

$$a_2 = [\beta/(\alpha_1\alpha_3)]^2 \, v_{grain}/15 \tag{52}$$

where α_1 and α_3 are to be specialized to the frazil parameters.

The next problem in evaluating (15) is the Green's function which satisfies (9) when $\underset{\approx}{K}_o$ has the form (17). It is not difficult to find the Fourier transform of $\underset{\approx}{\Gamma}$ [17]. An evaluation of the inverse transform yields

$$\underset{\approx}{\Gamma}(\underset{\sim}{r}) = \left(4\pi \, k_o^2 \, K_{01} \, K_{03}^{1/2}\right)^{-1} \nabla\nabla (e_1/r_K) + \underset{\approx}{\Gamma}_1 \tag{53}$$

where the nonvanishing components of $\underset{\approx}{\Gamma}_1$ are

$$(\Gamma_1)_{11} = e_o/(4\pi r) - \alpha\left[y^2 - x^2 + x^2\rho\frac{\partial}{\partial\rho}\right][e_1 - e_o] \tag{54a}$$

$$(\Gamma_1)_{22} = e_o/(4\pi r) - \alpha\left[x^2 - y^2 + y^2\rho\frac{\partial}{\partial\rho}\right][e_1 - e_o] \tag{54b}$$

$$(\Gamma_1)_{12} = (\Gamma_1)_{21} = xy\alpha\left[2 - \rho\frac{\partial}{\partial\rho}\right][e_1 - e_o] \tag{54c}$$

$$(\Gamma_1)_{33} = e_1/(4\pi K_{03}^{1/2} r_K) \tag{54d}$$

Here

$$\rho = [x^2 + y^2]^{1/2} \tag{55a}$$

$$r_K = [\rho^2/K_{01} + z^2/K_{02}]^{1/2} \tag{55b}$$

$$\alpha = i/\left(4\pi \, k_o \, K_{01}^{1/2} \, \rho^4\right) \tag{55c}$$

$$e_o = \exp[i \, k_o \, K_{01}^{1/2} r] \tag{55d}$$

$$e_1 = \exp[i \, k_o (K_{01}K_{03})^{1/2} r_K] \tag{55e}$$

Finally, turning to the integral in (15), note that (53) shows that $\underset{\approx}{\Gamma}'$ is a symmetric tensor. This combined with (40), (47), and (48) shows that the tensor $P_{i\ell} = C_{ijk\ell}\Gamma'_{jk}$ is symmetric. Its components are

$$P_{11} = [C_{1122} + C_{1212}]\Gamma'_{11} + [C_{1313} - C_{1212}]\Gamma'_{33} + C_{1212}\,\mathrm{Tr}\,\underset{\approx}{\Gamma}' \tag{56a}$$

$$P_{22} = [C_{1122} + C_{1212}]\Gamma'_{22} + [C_{1313} - C_{1212}]\Gamma'_{33} + C_{1212}\,\mathrm{Tr}\,\underset{\approx}{\Gamma}' \tag{56b}$$

$$P_{33} = [C_{3333} - C_{1313}]\Gamma'_{1313} + C_{1313}\,\mathrm{Tr}\,\underset{\approx}{\Gamma}' \tag{56c}$$

$$P_{12} = P_{21} = [C_{1122} + C_{1212}]\Gamma'_{12} \tag{56d}$$

$$P_{13} = P_{31} = [C_{1133} + C_{1313}]\Gamma'_{13} \tag{56e}$$

$$P_{23} = P_{32} = [C_{1133} + C_{1313}]\Gamma'_{23} \tag{56f}$$

where the symbol Tr means trace.

Thus, in view of the assumed exponential correlation functions (42) and (44), an evaluation of integrals involving components of $\underset{\approx}{\Gamma}'$ and exponential functions are necessary to evaluate $\underset{\approx}{E}$. We note immediately that terms involving Γ'_{12} will vanish because of the factor y in (54c) and the fact that $\underset{\sim}{k}$ has no y component (see (18)). Similarly, the $\nabla\nabla$ operation in (53) will lead to $E_{32} = E_{23} = 0$. These observations merely confirm the form (19) already deduced for $\underset{\approx}{K}$. For the remaining components, a preliminary integration by parts for those terms arising from $\nabla\nabla(e_1/r_K)$ in (53) is useful to allow an easy evaluation of the principal value required in (15). Letting $C(r)$ be either of the exponentials in (42) or (44) and recalling (11), it is found that

$$\begin{aligned} PV\int \exp[-i\,\underset{\sim}{k}\cdot\underset{\sim}{r}]C(r)\nabla\nabla(e_1/r_K)dV &= \int \exp[-i\,\underset{\sim}{k}\cdot\underset{\sim}{r}]C(r)\nabla\nabla(e_1/r_K)dV - \underset{\approx}{S} \\ &= \int \nabla\Big\{\exp[-i\,\underset{\sim}{k}\cdot\underset{\sim}{r}]C(r)\Big\}\nabla(e_1/r_K)dV - \underset{\approx}{S} \end{aligned} \tag{57}$$

because the integral over the surface at infinity vanishes. Since the singularity of $\nabla(e_1/r_K)$ is sufficiently mild, no particular precautions need be taken near the origin in evaluating the resultant integral.

Aside from easy integrals involving the terms $e_o/(4\pi r)$ in (54a) and (54b), it has not been found possible to evaluate the remaining integrals for $\underset{\approx}{E}$ in closed form. However, if spherical coordinates r, θ, ϕ are introduced, the ϕ integration leads to Bessel functions. The integrals of these with exponentials in r over the range from zero to infinity are tabulated integrals. Thus, only integrals over the range 0 to π in θ remain to be evaluated numerically. Because of their length, the formulas will not be written here although the equations already discussed make their derivation routine. They do not contain singularities and may be evaluated using Gauss quadrature formulas. The most difficult numerical situation arises at low frequencies for columnar ice of high salinity where K_{01} is significantly different from K_{03}. It has been found that a 10-point quadrature will result in errors much less than one part in a thousand for the components of $\underset{\approx}{K}$ at frequencies as low as 0.1 GHz.

VI. COMPARISONS WITH EXPERIMENTAL DATA

Most reported experiments on the dielectric constant of sea ice have treated a situation corresponding to a vertically propagating wave incident on a slab of ice oriented in its natural growth position. In the notation of this paper, $k_x = 0$ in (18). Thus the K_{22} component, which is equal to the K_{11} component because $k_x = 0$, of the tensor $\underset{\approx}{K}$ was measured. In a few cases [2], [18] additional measurements with the polarization of the electromagnetic wave parallel to what is called the z axis in this paper were made. Thus $k_z = 0$ and the K_{33} component was measured. In [2], further measurements were performed on ice samples cut at acute angles to the growth direction. Some complicated function of the components of $\underset{\approx}{K}$ was measured because both ordinary and extraordinary waves would be generated in the sample. Unfortunately, not enough details concerning the measurements were presented in these cases to allow a detailed analysis.

Experimental data from [1] on two samples of first-year ice denoted by FY 1-4 and FY 1-9 are considered first. Figures 1 and 2 show comparisons of computations based on the theory of this paper and measurements of the real and imaginary parts of K_{22} at two distinct temperatures. The computations use the salinity S and density ρ given in [1] together with an assumed mean brine cell angle $\theta_B = 24°$, correlation length ratio $\ell_z/\ell_\rho = 200$, a mean air bubble diameter $d_a = 0.49$ mm, a mean ice grain diameter $d_g = 1$ cm, and the expression (30) for S_{q1}, which is based on a cylindrical correlation function. If (27) is used for S_{q1}, the computed real parts are found to be slightly larger near 0.1 GHz and almost unchanged at 1 GHz but the computed imaginary parts are significantly larger (e.g., 1.7 versus 1.48 for FY 1-9 at $t = -5.2°C$) at 0.1 GHz. Even at 1 GHz, the use of (30)

instead of (27) results in a noticeable improvement of the fit for Im K_{22}. It is concluded that the low frequency data does not support the assumption of an elliptical equi-correlation surface for the brine cells. A comparison of the results shown in Figures 1 and 2 with the theories discussed in [1] and [5] show a considerably improved fit to the data. This is achieved with a more realistic brine cell length to diameter ratio. In fact, a ratio $\ell_z/\ell_\rho = 20$ such as used in [1] and [5] yields a poor fit to the experimental data.

Although K_{33} was not measured for these two samples, an examination of computed values of K_{33} with $k_z = 0$ is informative. It is found that K_{33} is considerably larger than K_{22} in the frequency range of Figures 1 and 2. For example, $K_{33} = 29.25+41.74i$ at 0.1 GHz and $5.64+3.37i$ at 10 GHz for the FY 1-9 sample at -5.2°C. Even for the FY 1-4 sample at -14.8°C, $K_{33} = 10.54+9.29i$ at 0.1 GHz and $3.48+0.51i$ at 10 GHz. At still higher frequencies, Re $K_{33}(k_x = 0)$ approaches Re $K_{22}(k_z = 0)$ not only for these cases but for all sea ice according to computations. For ice with a salinity greater than a few tenths ppt (parts per thousand), however, the imaginary parts of the components of $\underset{\approx}{K}$ differ measurably.

These computations are verified by a number of observations. Thus Sackinger and Byrd [18] have measured the dielectric constant of ice samples in the 26-40 GHz range. As an example, we consider their measurements on ice with a salinity $S = 7.2$ ppt in the temperature range -16.5 to -32°C. Essentially identical results were found for the real part of the dielectric constant whether the polarization of the electric field was perpendicular or parallel to the growth direction (K_{22} with $k_x = 0$ and K_{33} with $k_z = 0$ in the present notation). The ice density was not stated in [18]. However,

if $\rho = 0.83$ g/cm^3 is assumed, the computed Re K_{22} values at 26 GHz range from 3.12 at -16.5°C to 2.90 at -32°C in agreement with the reported values. Further the computed Re K_{33} is larger than these values by only 0.05 and 0.008 at -16.5 and -32°C respectively. Also, the computations show only an insignificant frequency variation of Re $\underset{\approx}{K}$ in the 26-40 GHz range. Again, this is verified by the data in [18]. The situation is different for Im $\underset{\approx}{K}$ and is summarized in Table 1. Unfortunately there was considerable scatter in the reported measurements so that only mean values and an indication of the scatter in the data is given. Computed values in the range 26-40 GHz are also shown in the table where the first number corresponds to 26 GHz and the second to 40 GHz. In addition to the above stated parameters, the parameters used in these computations are $\theta_B = 24°$, $\ell_z/\ell_\rho = 200$, $d_a = 0.5$ mm, and $d_g = 1$ cm. It is seen that the computations generally track the observations.

Other relevant experiments are discussed in [2]. Measurements on old ice with $S \approx 0$ ppt at a temperature of -13°C were made at frequencies of 3.79, 10, and 38.46 GHz. Because of the low salinity the measurements of Re K_{22} and Re K_{33} (corresponding to $\phi = 90°$ and $\phi = 0°$ respectively in the notation of [2]) showed essentially no anisotropy. Values were obtained in the range 2.5 to 2.7. Although no density information was given in [2], computations assuming $\rho = 0.7$ g/cm^3, which is reasonable for old ice, yielded values of Re K_{22} ranging from 2.51 to 2.59 between 3.79 and 38.46 GHz for $S = 0.05$ ppt. The largest difference between Re K_{33} and Re K_{22} was 0.005. These computations also assumed $\theta_B = 24°$, $\ell_z/\ell_\rho = 200$, $d_g = 1$ cm, and $d_a = 1.2$ mm. The assumed mean air bubble diameter is quite reasonable for old ice and yielded an attenuation

$$\alpha = 20\, k_o \log_{10} e\ \mathrm{Im}\ K^{1/2} \qquad (58)$$

(where K may be either K_{22} or K_{33}) of 2.01 dB/cm when $k_x = 0$ and 2.04 dB/cm when $k_z = 0$ for a frequency of 38.46 GHz. This is in agreement with the measured value of 2 dB/cm for each of the orientations. At 38 GHz, Im K_{22} is over 33 times greater than the quasi-static Im K_{022} so that the scattering contribution to $\underset{\approx}{K}$ is responsible for essentially the entire measured attenuation of this sample of ice. The attenuation at 3.79 and 10 GHz was too low to be measured. Computations show a small anisotropy at 10 GHz. The computed result for the K_{33} component is 0.05 dB/cm at 10 GHz which would appear to be difficult to measure based on the indicated system sensitivity [2].

Measurements on two samples of winter sea ice with salinities of 6.55 and 6.2 ppt at temperatures of -13 and -12°C respectively were also discussed in [2]. These samples showed considerably different behavior than the pack ice. Again, the ice densities were not given. Based on the rather large reported values of Re $\underset{\approx}{K}$, the assumption was made that $\rho = 0.9$ g/cm^3 with the other parameters required by the theory taken as $\theta_B = 24°$, $\ell_z/\ell_\rho = 200$, $d_a = 0.5$ mm, and $d_q = 1$ cm. Comparisons with the measurements are shown in Tables 2 and 3 for the two ice salinities. It is seen that the measured real parts are higher than computed values at 3.79 and 10 GHz. However, the measured difference Re K_{33}-Re K_{22} and the calculated difference Re K_{33}-Re K_{22} agree closely except for 10 GHz in Table 3 where no anisotropy is shown in the measurement. The high measured values do not appear to be consistent with the data in Figure 1 at 4 GHz and -14.5°C where, for a much higher salinity, a lower value of Re K_{22} was obtained. The calculated attenuation values

also show some points of agreement with the measurements although there are differences. There are too many unknowns to speculate as to the origin of these differences.

Another source of data, which is interesting because frazil is identified explicitly, will be examined. In [3], measurements at a frequency of 10 GHz were made on two samples of frazil as a function of temperature. Figures 3 and 4 show computed and measured results for Re K and Im K . According to the discussion in Sections IV and V, the propagation constant is independent of direction and polarization but the experiment did not attempt to verify this property. The computations assume $\ell_z/\ell_\rho = 200$, $d_a = 1$ mm, $d_q = 4$ mm in addition to the densitites and salinities stated in [3]. Notice that, at some temperatures, two measured values are shown. These correspond to measurements made during increasing and decreasing temperature cycles and provide some indication of the random experimental errors. Figure 4 shows that rather close agreement with the measured Im K values is achieved. Figure 3, however, indicates a consistent difference of about 0.2 between the measured and computed values of Re K over most of the temperature range. This difference is somewhat surprising - especially at temperatures below -20°C where the brine volume in ice of this salinity becomes negligible. The measured Re K values approximate those of pure solid ice, not porous ice with a density near 0.84 g/cm^3 which has a dielectric constant whose real part is near 2.87. On the other hand, the hydrated salts in the ice may have some unexpectedly large effects which are not treated as being substantially different from ice in the theory.

Data at 10 GHz on columnar and multiyear ice are also discussed in [3]. The two columnar ice cases are puzzling and not in accord with physical expectations. The ice with the higher density and higher salinity had a

measured Re K_{22} much lower than that of the lower density, lower salinity ice. Even its Im K_{22} value was lower for temperatures above -30°C. Both the higher salinity and higher density should have had the opposite effect. For the two multiyear ice cases in [3] the computed values of Re K_{22} are essentially the same and higher than the measured values by about 0.2. Lowering the assumed ice density to 0.73 g/cm^3 instead of the specified 0.77 g/cm^3 for the S = 0.61 ppt case brings the calculated values into agreement with the measurements at all temperatures. The calculated imaginary parts, however, are low by a factor of about 0.5. This may not be a problem because the scatter in the measured values indicate that high accuracy was not achieved in these measurements for such low Im K_{22} values.

VII. CONCLUSIONS AND RECOMMENDATIONS

A theory of the dielectric constant of sea ice has been developed which is able to account quantitatively for a large amount of published data in the frequency range 0.1 to 40 GHz.

However, some disagreements were noted. These may be due to a lack of quality in the data for there are apparent problems among some of the measurements themselves. The lack of really precise measurements shows, for example, in the data discussed with respect to Figures 1 and 2 where, even though the theory clearly reproduces the main observed characteristics, the experimental points do exhibit what must be assumed to be some significant random errors (the assumption that these correspond to real changes appears to be quite unreasonable and no known physical process could account for them). The large scatter in the experimentally determined imaginary part of the dielectric constant data discussed in connection with Table 1 was noted previously. This precluded a more quantitative check of the theory, which

generally falls within the reported range at each temperature, as a function of frequency for the particular data source in question. Bias type errors are also of some significance. For example the Re K_{22} measurements discussed in connection with Tables 2 and 3 at 3.79 and 10 GHz show a definite bias with respect to experimental data on approximately similar ice (FY 1-4) shown in Figure 1. The correction of this bias at 3.79 and 10 GHz, if it is real and the same for Re K_{33} as for Re K_{22} , would have resulted in significant improvement in agreement between the calculated and measured values of Re K_{33} as well as Re K_{22} .

These observations clearly show that dielectric measurement techniques for this difficult to measure substance must be developed further. Complete measurements require data not only for the case where the electric field polarization is perpendicular to the ice growth direction, but also parallel to it. As this report has shown, there is ample evidence that most forms of sea ice have anisotropic dielectric properties. Measurements at several frequencies and temperatures on a given sea ice sample should be mandatory. This procedure would greatly facilitate the comparison and checking of data from diverse sources since the large number of factors which influence the dielectric properties of sea ice would otherwise make intercomparison very difficult.

In addition to the dielectric constant measurements themselves, more care should also be exercised in reporting on such obvious physical properties such as density, salinity, and temperature. These play a major role in accounting for the dielectric properties even though, as seen in the discussion of the existing experimental data, they are not always given. A more subtle area is the specification of micro-structure statistics on such

features as air bubble size and brine cell length, dimension and orientation. These have not customarily been measured in connection with dielectric studies in the past but do seem to play a role. In fact, without these latter parameters, there is little hope of refining the theory since these have been shown to influence the dielectric properties. The lack of such published data required a number of ad-hoc assumptions in the present study.

REFERENCES

[1] M. Vant, R. Ramseier, and V. Makios, "The complex-dielectric constant of sea ice at frequencies in the range 0.1-40 GHz," J. Appl. Phys., Vol 49, pp 1264-1280, 1978.

[2] V. Bogorodskii and G. Khokhlov, "Anisotropy of the microwave dielectric constant and absorption coefficient of Arctic drift ice," Sov. Phys. Tech. Phys., Vol 22, pp 747-749, 1977 (English translation).

[3] M. Vant, R. Gray, R. Ramseier, and V. Makios, "Dielectric properties of fresh and sea ice at 10 and 35 GHz," J. Appl. Phys., Vol 45, pp 4712-4717, 1974.

[4] P. Hoekstra and P. Cappellino, "Dielectric properties of sodium chloride ice at UHF and microwave frequencies," J. Geophys. Res., Vol 76, pp 4922-4931, 1971.

[5] B. Farrelly, "Comment on the complex-dielectric constant of sea ice at frequencies in the range 0.1-40 GHz," J. Appl. Phys., Vol 53, pp 1256-1257, 1982.

[6] A. Stogryn, "The bilocal approximation for the effective dielectric constant of an isotropic random medium," IEEE Trans. Antennas Propagat., Vol AP-32, pp 517-520, 1984.

[7] E. Pounder, The Physics of Ice, New York: Pergamon, 1965.

[8] A. Assur, "Composition of sea ice and its tensile strength," in Arctic Sea Ice, publication 598, Nat. Academy of Sci. - Nat. Res. Council, Washington, D.C., 1958.

[9] A. Stogryn, "A study of the microwave brightness temperature of snow from the point of view of strong fluctuation theory," IEEE Trans. Geosci. and Remote Sens., to be published March, 1986.

[10] A. Stogryn and G. Desargant, "The dielectric properties of brine in sea ice at microwave frequencies," IEEE Trans. Antennas and Propagat., Vol AP-33, pp 523-532, 1985.

[11] K. Nelson, "A study of the freezing of sea water," thesis, University of Washington, Dept of Oceanography, 1953.

[12] G. Frankenstein and R. Garner, "Equations for determining the brine volume of sea ice from -.5° to -22.9°C, J. Glaciol., Vol 6, pp 943-944, 1967.

[13] A. Stogryn, "The bilocal approximation for the electric field in strong fluctuation theory," IEEE Trans. Antennas and Propagat., Vol AP-31, pp 985-986, 1983.

[14] A. Stogryn, "A note on the singular part of the dyadic Green's function in strong fluctuation theory," Radio Science, Vol 18, pp 1283-1286, 1983.

[15] A. Stogryn, "Correlation functions for random granular media in strong fluctuation theory," IEEE Trans. Geosci. Remote Sens., Vol GE-22, pp 150-154, 1984.

[16] H. Goldstein, Classical Mechanics, Cambridge: Addison-Wesley, 1953.

[17] H. Kogelnik and H. Motz, "Electromagnetic radiation from sources embedded in an infinite anisotropic medium and the significance of the Poynting vector," in Electromagnetic Theory and Antennas, pt I, New York: Pergamon, 1963.

[18] W. Sackinger and R. Byrd, "The dielectric properties of sea ice in the frequency range from 26 GHz to 40 GHz," IAEE Report 7203, University of Alaska, Fairbanks, Alaska, 1972.

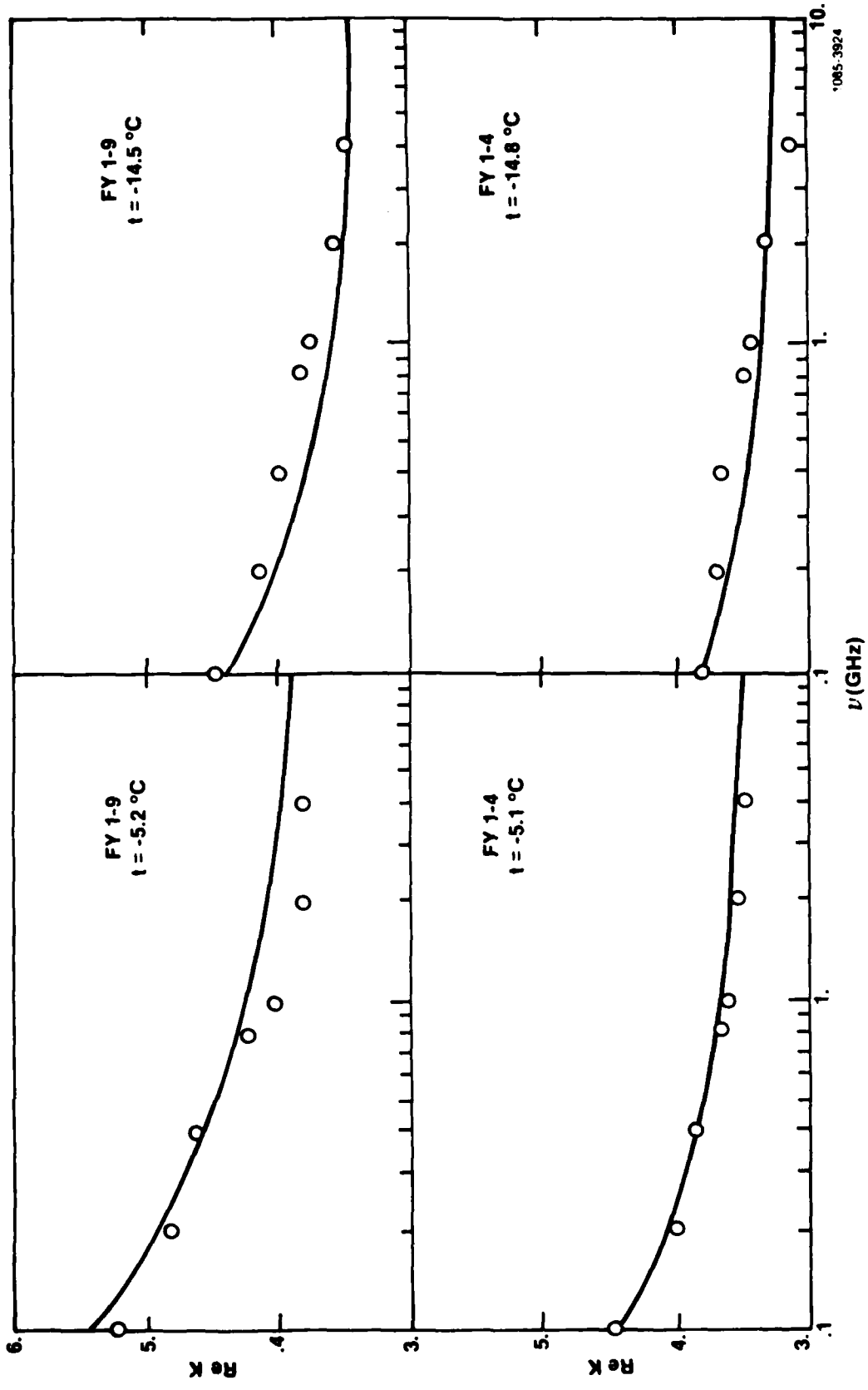

Figure 1. Real part of $K_{22}(k_x = 0)$ for first-year ice as a function of frequency. FY 1-9: $\rho = 0.91$ q/cm^3, $S = 10.5$ ppt. FY 1-4: $\rho = 0.91$ q/cm^3, $S = 5.1$ ppt.

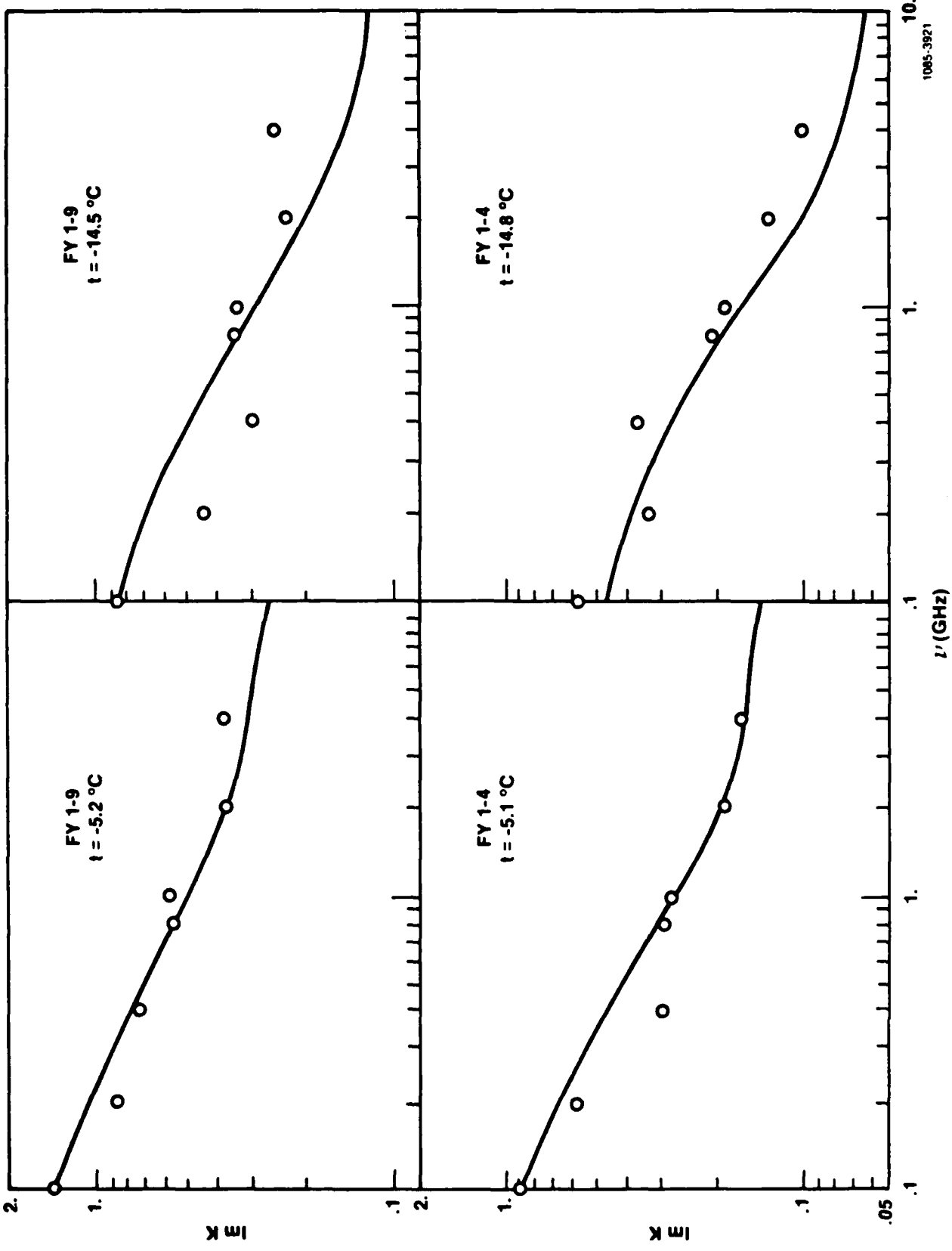

Figure 2. Imaginary part of $K_{22}(k_x = 0)$ for first year ice as a function of frequency. FY 1-9: ρ = 0.91 g/cm^3, S = 10.5 ppt. FY 1-4: ρ = 0.91 g/cm^3, S = 5.1 ppt.

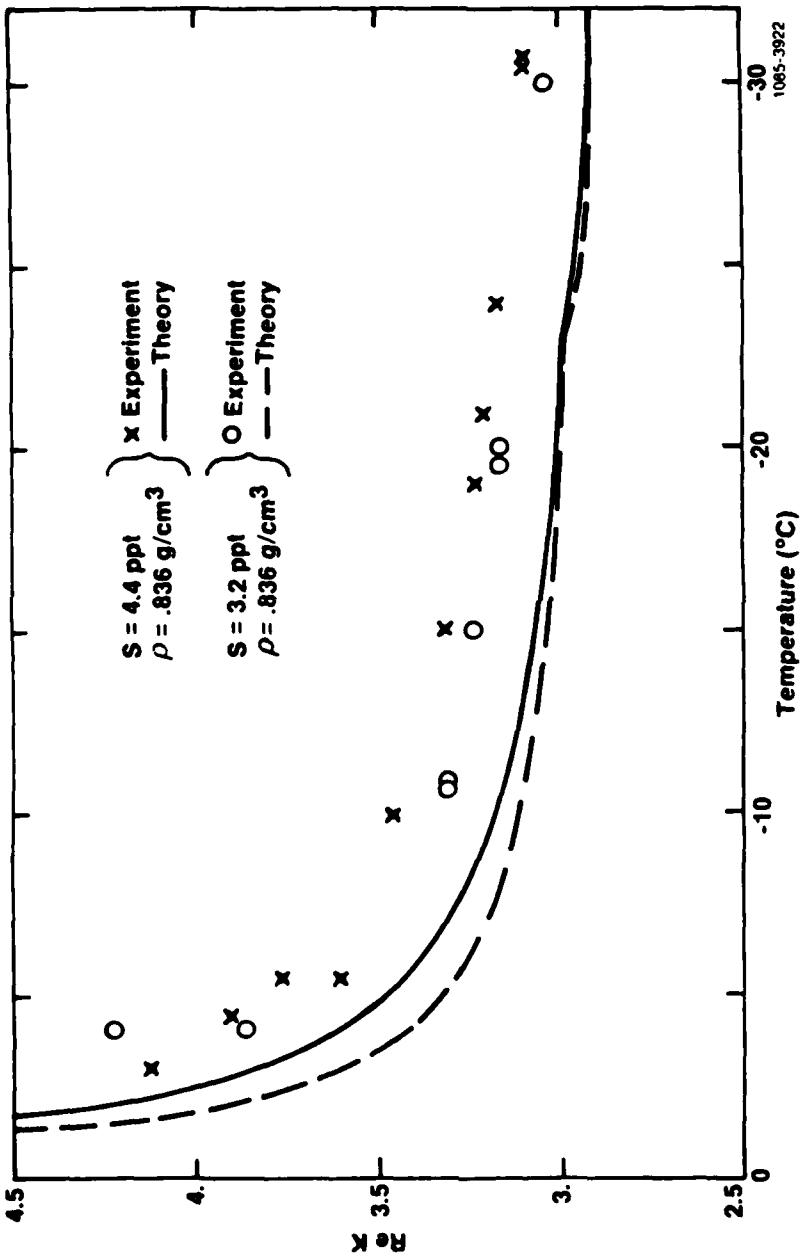

Figure 3. Real part of κ for frazil at 10 GHz as a function of temperature.

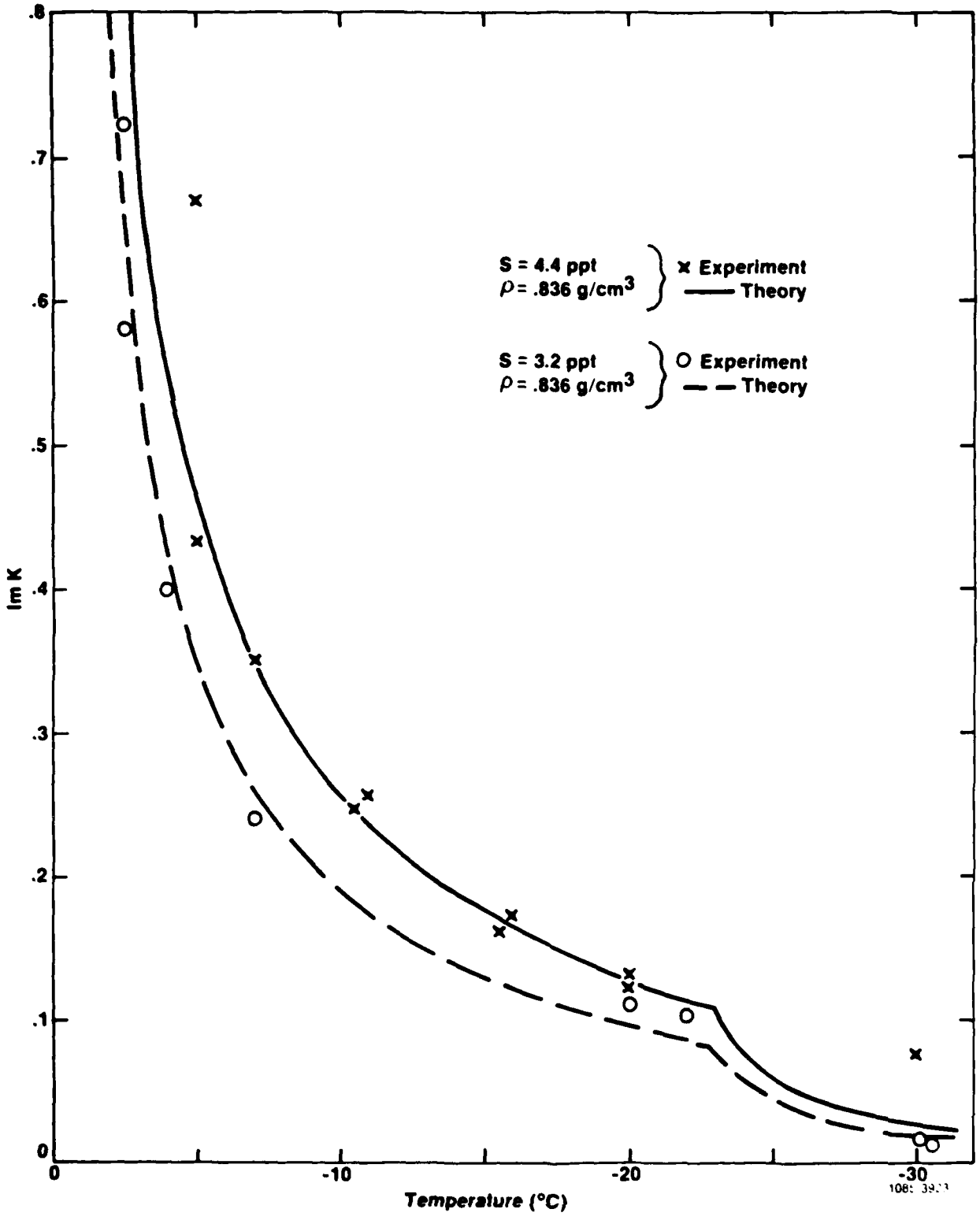

Figure 4. Imaginary part of K for frazil at 10 GHz as a function of temperature.

TABLE 1 COMPARISON OF CALCULATIONS OF THE IMAGINARY PARTS OF THE COMPONENTS OF K WITH MEASUREMENTS ON SEA ICE BETWEEN 26 AND 40 GHZ (S ≈ 7.2 ppt)

Temperature (°C)	Im K_{22}		Im K_{33}	
	Calculated	Observed	Calculated	Observed
-32.0	0.0168 to 0.0244	0.011 ±0.002	0.0397 to 0.0388	0.031 ±0.003
-25.0	0.0348 to 0.0409	0.045 ±0.015	0.110 to 0.0878	0.17 ±0.06
-21.5	0.0626 to 0.0668	0.054 ±0.025	0.225 to 0.168	0.19 ±0.06
-16.5	0.0780 to 0.084	0.084 ±0.036	0.320 to 0.237	0.22 ±0.06

TABLE 2 COMPARISON OF WINTER ICE (S = 6.55 ppt, t = -13°C)

DATA IN [2] WITH THEORY

Frequency (GHz)	Measured				Calculated			
			α(dB/cm)				α(dB/cm)	
	Re K_{33}	Re K_{22}	$k_z = 0$	$k_x = 0$	Re K_{33}	Re K_{22}	$k_z = 0$	$k_x = 0$
3.79	4.25	3.55	0.90	0.25	4.06	3.34	1.79	0.20
10.0	3.85	3.45	2.8	1.0	3.63	3.29	3.54	0.43
38.46	3.13	3.13	5.6	2.2	3.27	3.23	5.68	1.64

TABLE 3 COMPARISON OF WINTER ICE (S = 6.2 ppt, t = -12°C)

DATA IN [2] WITH THEORY

Frequency (GHz)	Measured				Calculated			
			α(dB/cm)				α(dB/cm)	
	Re K_{33}	Re K_{22}	$k_z = 0$	$k_x = 0$	Re K_{33}	Re K_{22}	$k_z = 0$	$k_x = 0$
3.79	4.6	3.9	1.1	0.2	4.01	3.32	1.71	0.19
10.0	3.8	3.8	3.0	1.2	3.60	3.29	3.37	0.42
38.46	3.1	3.2	5.2	2.8	3.26	3.23	5.41	1.56

END

DTIC

6-86

END

DTIC

6-86